processes

MDPI

Review

A Review of the Application of Discrete Element Method in Agricultural Engineering: A Case Study of Soybean

Dongxu Yan [1], Jianqun Yu [2], Yang Wang [2], Long Zhou [3], Kai Sun [2] and Ye Tian [4,*]

[1] Hua Lookeng Honors College, Changzhou University, Changzhou 213164, China; yandongxu@cczu.edu.cn
[2] School of Biological and Agricultural Engineering, Jilin University, Changchun 130022, China; yujianqun@jlu.edu.cn (J.Y.); ywang1987@jlu.edu.cn (Y.W.); sunkai20@mails.jlu.edu.cn (K.S.)
[3] School of Agricultural Engineering and Food Science, Shandong University of Technology, Zibo 255022, China; zhoulong18@mails.jlu.edu.cn
[4] Center of Industry and Technology, Hebei Petroleum University of Technology, Chengde 067000, China
* Correspondence: tianye0728@163.com; Tel.: +86-1871-3404317

Abstract: The discrete element method has become a common method for analyzing the contact interaction between particulate materials and between particles and mechanical components. It has been widely used in agricultural engineering and other fields. Taking soybean as an example, soybean seed particles always have contact effects between particles and mechanical components in the process of planting, harvesting, threshing, separation, cleaning, and processing. The discrete element method can be used to obtain information on the contact forces between seed particles and mechanical parts, as well as the velocity and displacement of seed particle motion from a microscopic perspective. This paper summarizes the application of the discrete element method in soybean cultivation and production processes in recent years. This will help future researchers to conduct relevant test studies, develop and improve existing research methods. It can also serve as a guide and reference for the production and processing of other granular materials and the optimization of agricultural machinery components.

Keywords: DEM model; soybean; contact model; soil; validation; coupling method

Citation: Yan, D.; Yu, J.; Wang, Y.; Zhou, L.; Sun, K.; Tian, Y. A Review of the Application of Discrete Element Method in Agricultural Engineering: A Case Study of Soybean. *Processes* **2022**, *10*, 1305. https://doi.org/10.3390/pr10071305

Academic Editor: Joanna Wiącek

Received: 26 May 2022
Accepted: 28 June 2022
Published: 1 July 2022

1. Introduction

The discrete element method (DEM) [1] is an effective method for analyzing and solving the problem of granular materials, which can be seen everywhere in agricultural production, for example, soil, seeds, particles, and so on. At present, DEM is widely used in agricultural engineering [2–8].

When analyzing the interaction between soybean particles, it is necessary to establish the geometric model of soybean particles, select the appropriate contact mechanics model, and determine the simulation parameters. So far, many domestic and foreign scholars have established the DEM model of soybean particles, and verified the model using different test methods.

When analyzing the interaction between soybean particles and soil particles, different types of particle materials are involved. Therefore, in addition to establishing the DEM model of soybean particles, it is necessary to establish the DEM model of soil particles. As is widely known, soil materials are very complex. Different scholars have established different DEM models of soil particles after analyzing the soil, and the contact models selected were mostly different. In particular, different contact models involve different simulation parameters, which play a crucial role in the simulation results, and scholars have used different test methods to calibrate and verify the relevant parameters.

When analyzing the motion of complex agricultural machinery, the DEM alone cannot achieve tasks such as the simulation of the working process of swing-bar sieves, deep-shovels, and seeding monomer. Coupling the DEM with other methods, such as coupling

the DEM with CFD, coupling the DEM with MBD, etc., can effectively solve the above problems.

2. Soybean Particle Modeling

There are many soybean varieties. When using the DEM to simulate and analyze soybean particles, scholars established the DEM model (geometric model and contact model) of soybean particles according to the shape and size characteristics of soybean varieties. The soybean varieties, and the geometric and contact models of soybeans selected by different scholars when conducting the above studies, are described below.

2.1. Geometric Model

(1) Circular and combined elliptical particle models

Shen established circular and combined elliptic particle models of soybean seed particles for two varieties, 1008 (sphericity of 93.4%) and Jidou 2 (sphericity of 94.7%), as research objects. The motion process of soybean particles inside the precision seed discharger was simulated and analyzed with the above two particle models, respectively, and the reliability of the analysis results of the DEM was verified by comparing the test and simulation results [9].

The circular and combined elliptical particle modeling methods are mainly applied using two-dimensional DEM. With the expansion of the DEM from 2D to 3D, this modeling method is rarely adopted.

(2) Single-sphere model

When using soybean particles with high sphericity as the research object, many scholars have approximated it as spherical particles for the purposes of analysis and research. At the same time, when using single-sphere models for simulation, the contact judgment algorithm between particles is simple, and the time cost can be saved to a great extent for the same number of particles.

Xu established a single-sphere model using two soybean varieties, Jidou 47 (sphericity of 91.3%) and Jidou 34-1 (sphericity of 94.8%). 2-D and 3-D DEM analysis and design software were used to simulate and analyze the impact of different factors (thousand grain weight, triaxial dimension, stiffness coefficient, friction coefficient, etc.) on the collision process of soybeans [10].

Zhang established a single-sphere particle model with three soybean varieties, Jike bean (sphericity of 91%), Jixin bean (sphericity of 90%) and Jidou (sphericity of 90%), as research objects. The metering process of a soybean seed metering device with an inner hole and type–hole wheel was analyzed by simulation, and a digital design method for a soybean seed metering device was preliminarily developed [11].

Yu et al. simplified soybean seed particles as spherical particles, taking Jike bean (sphericity greater than 88%) as the research object. Using self-developed 3-D CAE software, the metering performance of the metering device was simulated and analyzed. Compared with the test, the feasibility of DEM to analyze the type–hole wheel seed metering device was proved [12].

Lu et al. assumed that soybean seed particles were spherical particles and used a single sphere to build a soybean particle model to simulate the discharge process of an assembly of soybean particles in silo. At the same time, the flow rate and pressure of the particles in the discharge process were analyzed [13].

Nguyen et al. developed a single-sphere model using the Vietnamese DT84 variety of soybean as the study object. The relevant parameters of the DEM model were calibrated on the basis of a comparison of the tests and simulations, such as bulk density and silo discharge [14].

(3) Multi-sphere model

With the continuous application of the DEM in the field of agricultural machinery, the single-sphere model is no longer able to meet the requirements with respect to simulation

accuracy when studying the contact interaction between mechanical components and soybean particles. To express the geometry of soybean seed particles more accurately, for the modeling of soybean particles, a multi-sphere model has been gradually developed on the basis of the single-sphere model.

Vu-Quoc built a four-sphere model for soybean particles with a sphericity of 85.71%, and the four-sphere model was then employed to simulate the flow process of soybeans flowing down a chute with a bumpy bottom, proving that the simulation results were close to the test results [15].

Boac et al. developed one- to four-sphere models using soybean particles with a sphericity of 85.8%. By comparing the simulation and test of angle of repose and bulk density, it was proved that the simulation results of the one-sphere model were better than the two- to four-sphere models. In addition, the model was applied to the simulation analysis of soybean particle mixing problem in bucket elevator system [16,17].

Tao et al. approximated soybeans as ellipsoidal-shaped particles and developed three multi-sphere models of soybean particles. The applicability of the three models was analyzed from both macroscopic and microscopic aspects. The results showed that the simulation results of the three-sphere tangent model differed most from the test results, and the simulation results of the five-sphere model and the three-sphere intersection model were closest to the test values. Taking into account the computational time cost, the three-sphere intersection model was recommended for characterizing soybean particles with an ellipsoidal shape [18].

Liu et al. used four overlapping ball combinations to characterize the shape of soybean particles in the CATIA software. The diameter and coordinates of each ball were imported into the EDEM software, and the model was used to simulate and analyze the sowing process of soybean seeds under different conditions [19].

Xu selected four varieties of soybean seeds with different sphericities (86.91–96.02%) for a shape and size analysis. Moreover, Xu built multi-sphere models of 5-, 9-, and 13-sphere variations. Through the comparative analysis of the simulation and test by means of "self-flow screening" and "pilling", Xu found that the simulated results of the five-sphere model were close to the test results. However, the modeling scheme proposed by Xu, which did not optimize the position and radius of the constituent sphere, led to an increase in the error between the simulation results and the test results with increasing number of constituent spheres [20].

Yan selected 12 main soybean varieties from different regions of China, proving that the selected soybean seeds could be approximated to ellipsoid shape. Three varieties of soybean seeds with different sphericities (Suinong42, with a sphericity of 94.78%; Jidou17, with a sphericity of 86.86%; and Zhongdou39, with a sphericity of 80.6%) were then selected as examples. On this basis, 5-, 9- and 13-sphere models for soybean seeds with different sphericities were established. The applicability of the modeling method was verified by self-flow screening and angle of repose, in which the five-sphere model could be used when the sphericity of soybean seed particles is high, while the 9- and 13-sphere models could be used when the sphericity of soybean seed particles was low [21].

When using the multi-sphere model, the simulation results may be different from the actual situation due to the problem of multiple contact points.

Wang used a multi-sphere method to model maize kernels and simulated the falling and rebounding process of individual kernels with different numbers of contact points. The seed rebound height gradually decreases with the increase of the number of contact points. By changing the coefficient of restitution, the simulated rebound height at multiple contact points could be made to be equal to the simulated rebound height at a single contact point and the rebound height of the actual corn kernels [22].

Kodam et al. used a multi-sphere method to model spherical particles. On this basis, the collision process between a single spherical particle and the wall was simulated and analyzed. The contact force between the particle and the wall increased with increasing numbers of contact points. By changing the stiffness coefficient (Kc) and the power expo-

nent of overlap (n) in the contact model, the contact force at multiple contact points could be made to be equal to the contact force at a single contact point [23].

Kruggel-Emden et al. used the method of dividing the contact force by the number of contact points to make the contact force at multiple contact points equal to the contact force at a single contact point, which was used to reduce the effect of multiple contact points [24].

Zhou et al. used the Hertz–Mindlin (no-slip) model and the HM-new-restitution model (the HM-new-restitution model can appropriately reduce the effect of the multiple contact point problem) to study the effect of the multiple contact point problem on the simulation results of the assembly of maize particles. By comparing the simulation and test results of different multi-sphere models, it was demonstrated that the multi-contact points have less influence on the simulation results of the maize seed particle assembled [25].

Yan artificially constructed multi-contact points for a drop test of soybean seed particles by adjusting the coefficient of restitution so that the rebound heights of the particles were the same for different contact point cases. The results of the particle assembly simulation achieved using the above coefficients of restitution were essentially the same as the test results. This proved that the multiple contact points had a small effect on the simulation results of soybean seed particle assembly [21].

(4) Ellipsoid model

Related scholars have proposed algorithms for inter-particle collision detection for ellipsoidal particles. The ellipsoid equation method was used to directly model ellipsoidal particles [26–28]. Soybean particles can be approximated as ellipsoidal shapes, and whether an ellipsoid model of soybean particles can be directly established is related to the findings presented in the following studies.

According to Barr, the surface of a super-ellipsoid can be described by the so-called inside–outside function, as follows:

$$f(x,y,z) = \left(|x/a_i|^{s_2} + |y/b_i|^{s_2}\right)^{s_1/s_2} + |z/c_i|^{s_1} - 1 = 0 \quad (1)$$

where a_i, b_i and c_i are the half-lengths of the principal axes of the hypersphere particles, and s_1 and s_2 control the sharpness of the particle edges, which are called shape indices. When s_1, s_2 = 2, the equation can be expressed as an ellipsoid Equation (1) [29].

Ouadf et al. proposed a contact detection algorithm between ellipsoidal particles for simulating the mechanical behavior between ellipsoidal bodies. The algorithm was reliable in contact detection and was implemented in a modified version of the DEM program (Altair, Edinburgh, UK). The stress–strain–expansion curves obtained by simulating the compression using the improved procedure were consistent with the results [27].

You et al. used ellipsoid and multi-sphere models to describe ellipsoidal particles. Bulk density, dynamic angle of repose and silo discharge tests were carried out. The accumulation and flow characteristics of ellipsoidal particles were studied in simulations and tests. The results showed that the ellipsoid model was able to accurately reproduce the accumulation and flow behavior of ellipsoidal particles. In the simulation of the multi-sphere model, the accuracy of the simulation was acceptable when the number of constituent spheres was large, but the computation time was much longer than that of the ellipsoid model. When the number of constituent spheres was small, computation time could be saved, but the accuracy of the simulation decreased [30].

Yan et al. established the ellipsoid model of soybean particles after proving that soybean seed particles can approximate the ellipsoid shape. DEMSLab software was used to simulate the movement of particle groups, and the simulation results were compared with those of the multi-sphere model. The results showed that the simulation results of the multi-sphere model were closer to the test results. The reason for this was that the surface of the ellipsoidal particle model is smooth, while the surfaces of soybean seed particles are concave and uneven [31].

2.2. Contact Model

Renzo et al. used a linear model, a nonlinear model, and a nonlinear model with hysteresis to simulate and analyze the collision between the ball and the wall. At the macro scale, comparing the velocities of the particles after collision, the simulation results of the more complex contact model showed no significant improvement, and the linear model was better than the nonlinear model. At the micro scale, the tangential force, velocity, and displacement versus time obtained from the linear model simulation agreed better with the theoretical solution than the nonlinear model [32].

Boac et al. summarized the application of DEM in post-harvest grain modeling. The linear contact model and the Hertz–Mindlin contact model have been widely and effectively used to study grain handling and processing operations [16].

Landry H. et al. proposed a calibration method based on a virtual shear to determine the properties of fertilizer. The influence of parameter sensitivity of linear and Hertz–Mindlin contact constitutive model was studied. The results showed that many parameters affected the performance of fertilizer particles in the shear test [33].

Gao developed a coupled three-dimensional isogeometric/DEM to model the contact interaction between structures and particles. Taking the impact of a small ball on thick plate as an example, linear models, Hertz contact models and quadratic models were studied. The results showed that the Hertz contact model exhibited the best behavior, as the interaction law between a sphere and an isogeometric element within the elastic range and no additional correction factors was required [34].

Horabik et al. studied the collision between crop seed particles (peas, soybeans, and canola) and flat plates at different moisture contents using the Visco-elastic contact model based on Hertz contact theory. The results showed that the model provided a very good approximation of COR (V0) and impact time tc (V0) relationships, and a sufficiently good approximation of the shape of Fn(t) relationships [35].

The above summary shows that for non-viscous and elastic crop material particles, the main contact models used to study the interaction between particles and between particles and boundary materials are linear models, a nonlinear model, Hertz models, Hertz–Mindlin models, visco-elastic contact models, etc. In the analysis of the interaction between soybean seed particles and between soybean and mechanical components, the choice of which contact model to use needs to be carefully analyzed.

2.3. Validation of Particle Models

Most of the test validation methods used by different scholars for the DEM simulation of particles have been different, and the test and simulation methods that have commonly been used for particle model simulation calculations in recent years are described below.

(1) Bulk density

Chen et al. used a Winchester cup to measure the bulk density of grains, as shown in Figure 1a, where grains were placed in a funnel with a sliding door at the bottom of the funnel. The grains in the top funnel should be of sufficient quantity to ensure that the cup overflows when it is full. The grains on top of the cup need to be scraped off with a wooden scraper.

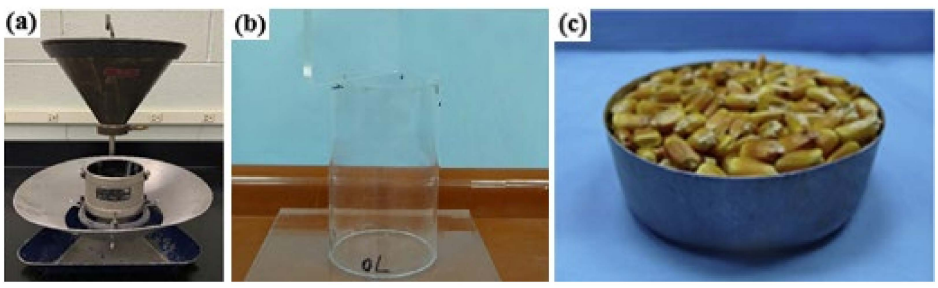

Figure 1. Bulk density apparatus.

The calculation of bulk density can be expressed as

$$\rho = \frac{m_1 - m_0}{V_{cup}} \tag{2}$$

where $m_1 - m_0$ is the mass of particles in the cup after scraping and V_{cup} is the volume of the cup. In the simulation, assuming a small overlap between the particles, the porosity can be calculated as

$$\varphi_{sim} = \frac{V_{void}}{V_{cup}} = \frac{V - V_{Kernel}}{V_{cup}} \tag{3}$$

where V_{void} is the volume of the void space and V_{Kernel} is the total volume of all particles in the cup. In the simulation, the porosity can be expressed as

$$\varphi = 1 - \frac{\rho_b}{\rho_p} \tag{4}$$

where ρ_b is the packing density, ρ_p is the particle density [36].

Zhou et al. conducted a bulk density using the apparatus shown in Figure 1b. The accuracy and applicability of the particle model were verified by comparing the simulation and test results [25].

Wang et al. used the apparatus shown in Figure 1c to conduct a bulk density test with maize seed particles in a cylindrical-shaped aluminum box. A comparison of simulation and test results was used to verify the feasibility and validity of the maize particle model and the maize particle population model [37].

(2) Angle of repose

Chen et al. used maize and wheat as research objects for the angle of repose using the apparatus shown in Figure 2a. The results showed that the simulation and test angle of repose results were relatively close [36].

Mousaviraad et al. used the apparatus shown in Figure 2b to perform angle of repose and also simulated and analyzed the angle of repose for different numbers of constituent spheres. The parameters of the maize particle model were calibrated by comparing the test and simulation results [38].

Wang Yang et al. used the apparatus shown in Figure 2c to perform angle of repose tests. The accuracy of the multi-sphere particle model was verified by comparing the simulation and test results of the angle of repose size and formation time [39].

Liu used the test device shown in Figure 2d to conduct angle of repose tests. By lifting the cylinder at a constant speed, the wheat seed particles formed an angle of repose on the organic glass plate. Comparing the test and simulated angle of repose, the simulation parameters were calibrated using the response surface method [40].

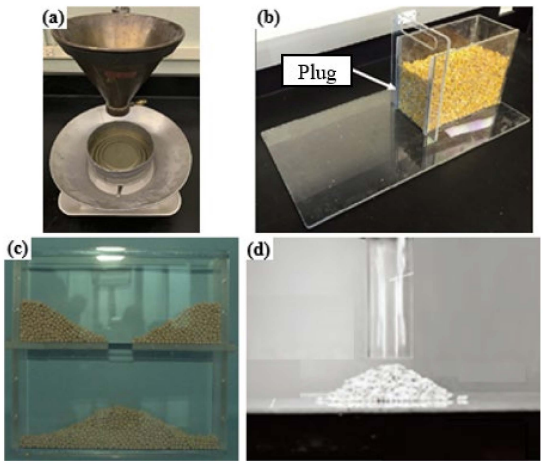

Figure 2. Angle of repose device.

(3) Dynamic angle of repose

Coetzee et al. used the dynamic angle of repose device shown in Figure 3 to calibrate the friction coefficient of particles with enlarged and unenlarged sizes. The rotating drum diameter was greater than or equal to 25 times the particle diameter. The speed of the rotating drum was 4.8 rpm. The simulation results showed that when the magnification factor of particle size was less than 4, the simulation results of the dynamic angle of repulsion were accurate; when the magnification factor was greater than 4, the simulation results were inconsistent with the results [41].

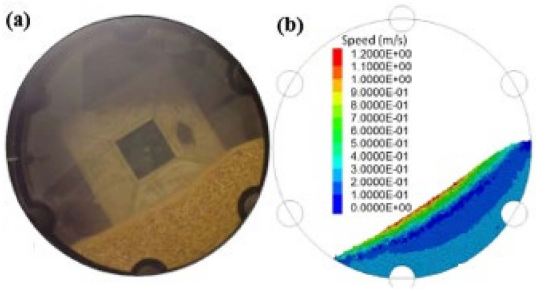

Figure 3. Corn seed particle dynamic angle of repose. (**a**) Test device diagram; (**b**) simulation diagram.

Cunha et al. explored a dynamic angle of repose using the device shown in Figure 4. A rotating drum was filled with soybean seed particles, and when the drum was rotated at a constant angular velocity, the soybean seed particles were in a relatively stable state, forming a dynamic angle of repose. Image processing was used to measure the magnitude of the dynamic angle of repose. Analysis of the simulation and results showed that the static friction coefficient and rolling friction coefficient have a large effect on the dynamic angle of repose [42].

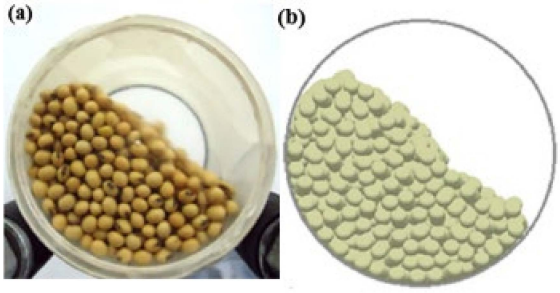

Figure 4. Soybean seed particle dynamic angle of repose. (**a**) Test device diagram; (**b**) simulation diagram.

Han et al. studied the effect of shape approximation on simulation results with static and dynamic angle of reposes using seven multi-sphere models with rice particles as the object. The analysis showed that in order to improve the simulation accuracy, different tests require different degrees of shape approximation. The dynamic angle of repose of the rice particle model decreased with increasing shape approximation, which was similar to the trend of the static angle of repose. However, for the same degree of shape approximation, the dynamic angle of repose was significantly larger than the static angle of repose [43].

(4) Silo discharge

Coetzee et al. established a rectangular flat-bottomed silo, as shown in Figure 5. The flow shape and flow rate of the granular material during silo discharge were studied. The simulation and test had the same trend of particle flow shape in the same time; the flow rate was slightly higher in the DEM simulation results obtained on the basis of the statistics

of the flow rate. When the flow rate was higher, the simulation results were more accurate with a larger silo opening [44].

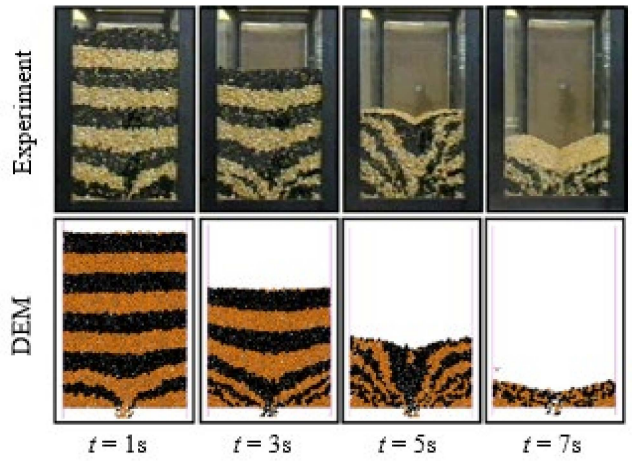

Figure 5. Test and simulation diagrams of rectangular flat-bottom silo.

Xu et al. conducted a rectangular flat-bottom silo discharge test and performed a statistical analysis of the flow shape and flow rate of LiaoDou 15 soybean seed particles. From the perspective of flow shape, the flow shapes of the simulation and the test were basically the same; with respect to flow rate statistics, the five-ball model simulation results were closer to the test values [45].

You et al. studied the discharge process of ellipsoidal particles in a flat-bottom discharge silo. The simulations of the multi-sphere model and the ellipsoid model had high similarity to the test with respect to the flow shape, but the analysis of the flow rate showed that the discharge curve of the ellipsoid model was closer to the corresponding test results. Therefore, the ellipsoid model was able to more accurately reproduce the flow behavior of ellipsoidal particles in the flat-bottom silo compared with the multi-sphere model [30].

Gonzalez-Montellano et al. applied different DEM models to simulate the discharge process of glass beads and corn particles in a conical-bottom silo. The mean bulk density, discharge time and flow shape during filling were analyzed and compared. The results showed that the simulation results of the glass bead DEM model were acceptable, and the simulation results of the corn model were problematic. Acceptable simulation results could be obtained by modifying the friction coefficient in the model [46].

(5) Self-flow screening test

Wang Yang et al. conducted a self-flow screening test of soybean seeds using the test apparatus shown in Figure 6. Comparison of the simulation and test results showed that the simulation results of the percentage passing of the five-sphere model were closer to the test values. The feasibility and effectiveness of their proposed five-sphere model modeling method for soybean seeds were initially demonstrated [39].

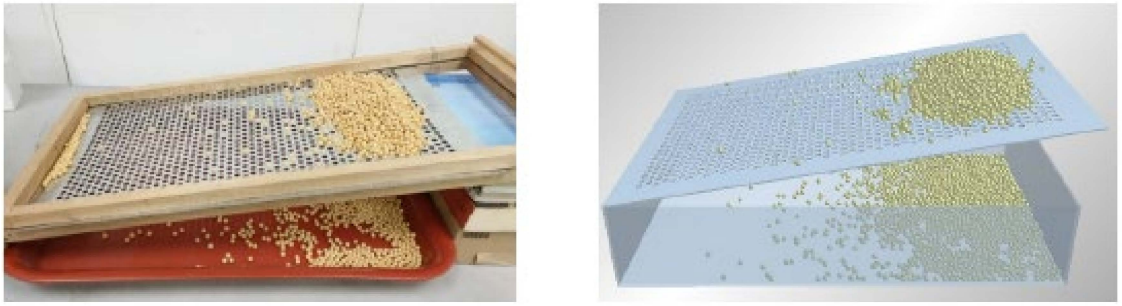

Figure 6. Test and simulation diagrams of self-flow screening.

Chen et al. used the same self-flow screening device. The self-flow screening test of corn seed particles was carried out under different sieve aperture sizes and inclination angles. The accuracy of the proposed corn seed particle modeling method was verified by comparing the simulation and the test results [47].

Zhou et al. similarly conducted self-flow screening tests. The simulation analyzed the sieve permeability process of the maize seed particle model with different numbers of constituent spheres, and the simulated percentage passing results were compared and analyzed with the test results to verify the applicability of their established particle model [25].

(6) Rotating cylinder mixing test

Cai et al. used the rotating cylinder test shown in Figure 7 to validate the spherical particle model. A high-speed camera was used to record the particle flow process, and each recorded image was processed by an image processing program to identify the position and color of each particle on the surface and calculate the mixing index. The simulation and test results were in good agreement, which proved that the DEM model it built was able to reasonably reproduce the mixing and flow situation of spherical particles in a rotating cylinder [48].

You et al. studied the mixing process of ellipsoidal particles in a rotating cylinder and established a multi-sphere model and an ellipsoid model for ellipsoidal particles. By analyzing the mixing index of particles in different particle models, the ellipsoid model was able to accurately reproduce the mixing of particles [30].

Liu et al. simulated the lateral mixing of wet particles in a rotating cylinder. The results showed that the mixing rate of particles generally decreased with increasing surface tension and filling rate. However, the mixing rate was the worst at a filling rate of 64% [19].

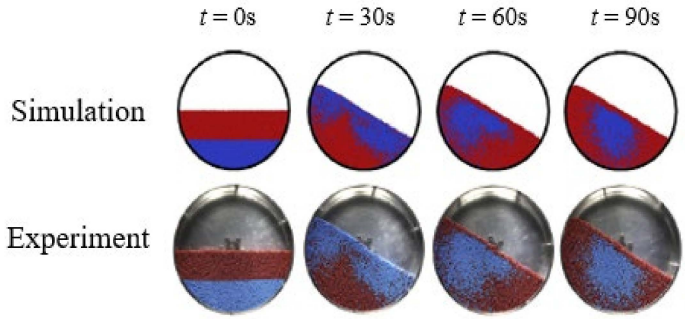

Figure 7. Simulation and test diagram of rotating cylinder mixing test.

Ma et al. studied the flow characteristics of ellipsoidal particles in a horizontal rotating cylinder using the DEM method. At low rotational speeds, the mixing of different types of ellipsoidal particle models was approximated. At high rotational speeds, the closer the shape of the ellipsoidal particles to spherical, the higher the degree of mixing; the degree of mixing of long ellipsoidal particles was slightly higher than that of flat ellipsoidal particles [49].

The above summary shows that the test methods used for particle model validation and simulation analysis include the bulk density test, angle of repose test, dynamic angle of repose test, silo discharge test, self-flow screening test, and rotating cylinder mixing test. Scholars can choose the appropriate validation methods according to their actual needs.

Currently, DEM models for soybean particles are all relatively mature. Scholars should select or develop accurate particle modeling methods according to their research objectives.

3. Soil Particle Modeling

Crops cannot be grown without soil, but the texture of soil varies from region to region. In analyzing the interaction between soil particles and between soybean seeds and soil by DEM, it is necessary to establish appropriate DEM model for testing soil particles in addition to establishing DEM model for soybean seed particles.

3.1. Geometric Model

Songul et al. established a sphere model of soil particles with a diameter of 10 mm to generate an assembly of soil particles in a uniformly distributed manner. The displacement of soil particles was simulated during the work of the sweeps. In most cases, the displacement of the simulated soil had a similar trend to that of the measured values. Comparing the simulation and test results of the average and maximum displacements of the soil, there were only a few cases where the relative error was less than 20% [50].

Ucgul et al. developed a sphere model of soil particles. The radii of the sphere model were taken as 4 mm, 5 mm, 6 mm, 7 mm, 8 mm, 9 mm, and 10 mm. The soil particle population was randomly generated, with a size distribution in the particle size range of 0.95–1.05 times the current particle size. The results showed that using larger particle sizes gave appropriate results while also speeding up the DEM simulation [51].

Ucgul et al. established a sphere model of soil particles with a radius of 10 mm, and analyzed the soil after plough tillage. The results showed that the simulated values of lateral and forward movement of surface soil were larger than the measured values, and the simulation of deep soil agreed well with the test results [52].

Bravo et al. developed a sphere model of soil particles to simulate a soil direct shear test. Particle models with different particle sizes (3–4 mm in the surface layer, 4–6 mm in the middle layer, and 6–8 mm in the bottom layer) were used to fill the soil bin, and soil tillage in hard-dry, soft-wet, and friable states were simulated and analyzed, accordingly [53].

Zhang performed a uniaxial compression test of soil using a sphere model with a particle size of 1 mm for simulation. The comparative analysis of pressure–strain curves showed that the simulation and test trends were similar. On this basis, the influence of different mechanical forward speed, rotary blade speed, cover grid, and rotary blade position on soil throwing performance was simulated and analyzed [54].

Pan established single-sphere, double-sphere, horizontal three-sphere, and triangular three-sphere particle models after analyzing the shape of soil particles. The working condition of the core-type opener in soil bins was simulated and analyzed. The reliability of the simulation results was verified by comparing the simulation results with the bench test [55].

Yan used a particle analyzer to observe and analyze the test soil. The soil particles were classified into sphere-like particles and triangular-like particles, while the 1- and 3-sphere models of soil particles were established. The relevant parameters were determined by test and simulation [56].

3.2. Contact Model

The selection of a contact model for the contact between soil particles is different from that for soybean seed particles. It mainly depends on the texture of the soil particles. The contact models proposed or selected by domestic and foreign scholars in the study of cohesive soil particles are described below.

Milkevych et al. established a parallel bond model to study the soil displacement caused by the interaction between soil and agricultural machinery components during deep loosening. The DEM model of cohesive soil with parallel bond contact between soil aggregates was established. A simulation of the mechanical tests was conducted, as well as simulation analysis and test research on the interaction between soil and agricultural machinery components in the process of deep loosening [57].

Chen et al. conducted deep loosening tests and simulations on three different soils (coarse sand, loam, and sandy loam) using a parallel bond model (PBM). Simulation and test results of soil cutting forces and soil disturbance characteristics caused by deep loosening were compared and analyzed. The results showed that the relative error was less than 10% in most cases [58].

Martin et al. proposed a DEM model to simulate cohesive soils. A single spherical particle was used to model the geometry of the soil particles with a random particle size distribution. By adding additional damping coefficients to suppress it is rolling. The

macroscopic mechanical property parameters of the actual soil were used as the parameters of the model [59].

Ma et al. used the Edinburgh model to simulate and analyze the tillage process of a convex round-blade deep loosening shovel. The effect of different tillage depths and speeds on tillage resistance and the drag reduction effect of the deep shovel were analyzed. The accuracy of the soil particle model and the rationality of the design of the convex round-blade deep loosening shovel were verified [60].

Wang et al. used The Edinburgh Model as a soil particle contact model. Tire–soil compaction simulation tests were conducted, and it was found that the difference between the simulated and measured stress values at the tire–soil contact surface were low. It was proved that the ECM contact model was consistent with the constitutive relationship of soil [61].

Xiang et al. used the Hertz–Mindlin with JKR model (JKR model) to analyze clay loam soils in southern China. The parameters of the JKR model were calibrated by angle of repose tests. The accuracy of DEM model to reflect the physical and mechanical properties of soil was verified by comparing the simulation of hole- forming with the soil bin test [62].

Wu et al. selected the JKR model as the contact model in consideration of the cohesive force between soil particles. The parameters involved in this model were calibrated using an angle of repose test. Simulations were performed using the calibration parameters and compared with the tests to demonstrate the accuracy of the calibration parameters [63].

Shi et al. studied the northwest agricultural soil and integrated the hysteretic spring contact model and liner cohesion model into a combined contact model. Next, the simulation parameters were calibrated using an angle of repose test. Comparing the simulation and test results, the combined model was proved to be feasible [64].

3.3. Parameter Calibration

There are many parameters in the contact model during soil particle simulation. The parameters that cannot be measured by test methods need to be calibrated. The tests used to calibrate the parameters between soil particles are mainly the bulk density test, the cone penetration test, the angle of repose test, the compression test, and the shear test; Figure 8 shows a screenshot of these test simulations.

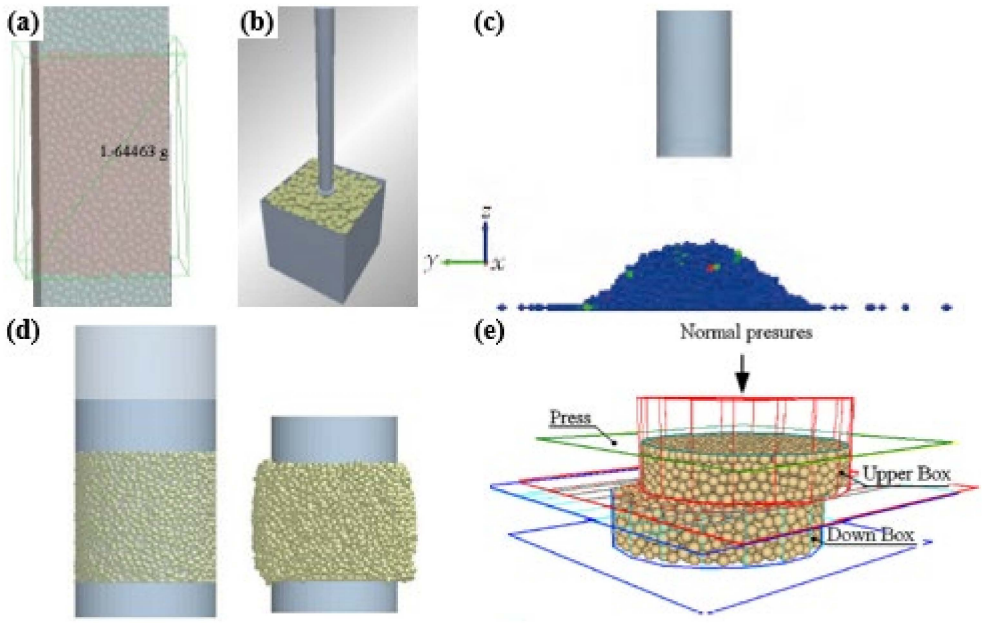

Figure 8. Simulation screenshot of (**a**) bulk density test, (**b**) cone penetration test, (**c**) angle of repose test, (**d**) compression test, and (**e**) shear test.

Ucgul et al. determined the DEM parameters required to simulate soil tillage processes by means of angle of an repose test and a cone penetration test. The results showed that when the appropriate contact model and parameters were adopted, DEM could effectively predict the interaction force between non-cohesive soil and tools, and simulate the movement of soil particles [51].

Mohammad et al. developed a DEM model using the PFC simulation tool. The shear test of the soil was simulated, and the shear behavior of the soil was predicted according to the relationship between shear stress and displacement. The model parameters were calibrated, and the effects of soil moisture content and bulk weight on the shear properties of sandy soils were studied [38].

Bravo et al. obtained the macroscopic parameter values of the mechanical properties of soil using a shear test. The values of parameters such as elastic modulus, shear strength, friction coefficient and cohesion of the soil were obtained using statistical regression equations. The accuracy of the model was also verified by comparing the simulation and test results on the basis of soil bin tillage tests [53].

Xie et al. calibrated the relevant parameters of the Edinburgh model by uniaxial compression test and unconfined compressive strength test. Since there were many simulation parameters, the sensitive parameters were first determined using the Plackett-Burman test, and then the sensitive parameters were calibrated using the quadratic orthogonal rotation combination test. Finally, the parameter calibration results were verified [65].

Li et al. studied two soils with different moisture contents using the JKR model. The simulation parameters were calibrated using the angle of repose test and optimized using the response surface method. The simulation results of the optimized parameters were similar to the test results, which proved that the model and parameter calibration were accurate [66].

Wang et al. determined the DEM parameters of loose cohesive soil modeled using hysteretic spring and linear cohesion contact models by a combination of Plackette Burman, steepest ascent and central composite tests [67].

Lin et al. used a cohesive contact model to simulate the forces between the soil particles, verifying the mixing effect of this mixer on cohesive materials. The effects of filling level, rotating shaft speed and size, particle cohesion and size on particle dynamics, and mixing performance within the mixer were investigated [68].

The above provides an overview of modeling methods for soil particles, contact models commonly used in soil particle simulation, and test methods for calibrating parameters. When establishing a soil particle model, scholars can choose according to the type of test soil. Meanwhile, for the DEM model of soil particles, ambiguities regarding the particle model, the number of particles, and the simulation time are urgent problems to be solved. Additionally, due to the complexity of soil particles, the calibration of particle parameters needs to be studied in depth.

4. Analysis of Soybean-Soil Contact

4.1. Seed Throwing Test

For the seed throwing test, scholars mainly compare the position of seeds at rest after collision with the position at the time of collision, and analyze the effect of different factors on the change of seed particle position.

Bufton et al. described the trajectories of different seeds released from the metering mechanism through tests. The seeds impacted the soil surface at known impact velocities and angles, and the displacement of bounce and rolling after rebound were measured. The test results showed that the impact velocity and angle, soil surface properties, and seed types affected the average displacement. The minimum displacement occurred at low impact velocities and impact angles between 75 and 85°. The displacement of the shear surface was smaller than that of extrusion surface, and the displacement of small irregular seeds was smaller than that of spherical seeds [69].

Ma et al. used a photoelectric sensor to measure the seed landing velocity, and further measured the bounce and rolling displacement after seed collision. A mathematical model of bounce and rolling displacement after seed bounce was established. The bounce and rolling displacement of the seeds simulated using the model followed the same trend as the actual measurements, proving that the model was accurate [70].

Ma established a mathematical and statistical model for seed distribution during precision sowing on the basis of Precision Sowing Theory, predicted the plant distribution in the field, and proposed the sowing method known as "encrypted precision sowing" [71].

Wang et al. established a mathematical model of grain spacing, derived the grain spacing distribution, and performed a distribution fitting test using the measured grain spacing samples. The test results fitted well with the results calculated using the mathematical model, confirming that the grain distance distribution model was valid, credible and feasible [72].

Sui conducted a sowing test to count the deviation of soybean seed particles. On the basis of analysis of the test results, the final drop point of the seeds was studied under different rotational speeds of seeding shaft, seeding height, conveyor belt speed and soil moisture content. At the same time, EDEM software was used to simulate some test processes, thus verifying the feasibility of the simulation of the seeding process [73].

Yan analyzed the effects of throwing height, soil plane inclination, collision orientation, and throwing speed on the bouncing and rolling distance of soybean particles using a high-speed camera. After calibrating the relevant parameters by angle of repose test, the above tests were simulated, and the results showed that the simulation and test results were in good agreement [56].

4.2. Calibration of Soil-Seed Parameters

When conducting seed throwing test, the main object of study is the collision between soybean seed particles and soil particles. When using the DEM software to simulate the above test, the material properties of the two kinds of particles are different. Domestic and international studies relevant to how the parameters between the different particle materials should be calibrated are described below.

Hao et al. developed a DEM model of yam along with a soil particle model. The soil–yam particle interactions were calculated using the JKR model. The restitution coefficient, static friction coefficient and rolling friction coefficient between the soil and the yam particles were calibrated by drop test, sliding test and rolling test, respectively [74].

Xu studied the interaction between soybean and soil particles using JKR contact model. In the simulation, the restitution coefficient was measured by drop test, and the static friction coefficient and rolling friction coefficient were obtained by calibration. The surface energy between soil and soybean particles was the same as that between the soil particles [45].

Yan used Edinburgh model simulation to analyze the collision between soybean and soil particles. The parameters between the soil particles and the soybean particles were calibrated on the basis of an angle of repose test, and the accuracy of the parameter calibration was demonstrated by comparing the simulation and test results [56].

From the previous review, it is clear that there have been few analyses of the seed throwing process, especially regarding the methods for calibrating the parameters between particles with different material properties; therefore, more in-depth studies and analyses are needed regarding seeding tests.

5. Coupling of DEM with Other Algorithms

Many complex mechanical motions cannot be simulated using the DEM alone, so scholars have adopted methods where the DEM is couples with other algorithms to analyze complex mechanical motions.

Dowding et al. developed a model in which the DEM and the FEM were coupled. The influence of the frequency and wavelength of propagating sinusoidal waves on the relative shear displacement of a jointed rock slope was studied [75,76].

Mark et al. used the DEM to describe the mechanical properties of soil particles and the FEM to represent the tire tread. The coupling method made it possible for the two regions to be effectively combined. The traction characteristics of the tire–ground interaction were simulated, and a comparison with the test results showed that the coupling algorithm was accurate [77].

Ding Li et al. used coupled the DEM and CFD algorithms to analyze the variation law of type–hole pressure during seed rower operation. The operation of the seed rower under normal operating speed was simulated and compared with the test for analysis [78].

Ren et al. used the DEM model to simulate particle motion, and the k-ε two-equation turbulent model to simulate gas motion. A two-way coupling numerical iterative scheme was used to incorporate the effects of gas–particle interactions in terms of momentum exchange, and investigated the flow of corn-shaped particles in a cylindrical spouted bed with a conical base [79].

Wang analyzed the simulation and test results of the sieving process of a pendulum screen based on the coupled DEM and MBD algorithms using AgriDEM software developed independently by the Digital Design Laboratory of College of Biological and Agricultural Engineering, Jilin University [80].

Xu simulated the working process of a coverer and a roller based on the coupling algorithm of the DEM and MBD using EDEM software coupled with ADAMS software. The feasibility and applicability of the coupling method were verified by comparing the displacement of the seeds during the simulation and the test [45].

Yuan et al. established a self-excited vibration deep loosening machine soil system model based on a coupling of the DEM and MBD algorithms. AgriDEM software was used to simulate and analyze the interaction between the mechanical components and the soil particles, and the accuracy of the model was verified [81].

Yan analyzed the working process of seeding monomer using EDEM software coupled with RecurDyn software based on the coupling algorithm of DEM and MBD. By comparing the test and simulation results, the opening angle, the position deviation of seed particles and the uniformity of grain spacing under different working speeds were analyzed [56].

Zhang et al. analyzed the subsoil mechanism process acting on the soil through a co-simulation using ADAMS–EDEM, and compared the results with those for the common subsoiler. The results showed that the soil modeling method in which the plow pan is created separately and a preset force extrusion is used was accurate and effective [82].

The coupling of the DEM with other methods, mainly including the coupling of DEM with CFD and the coupling of DEM with MBD, was reviewed in our previous paper. Coupled algorithms are currently becoming more widely used; but for researchers, the interactions between different software programs are required to analyze problems, which undoubtedly increases the difficulty and complexity of the research. Therefore, scholars in this field require further research to be done into the development of simulation software in order to afford a more in-depth study of DEM.

6. Conclusions

This paper focuses on the application of the DEM in the field of agricultural engineering, and reviews the application of the DEM in the planting and harvesting process of soybean in recent years, including the modeling of the particle materials, the selection of the contact model, model validation, the calibration of parameters, and the coupling of the DEM with other algorithms. The main conclusions are as follows.

(1) For soybean particle modeling, from 2-D to 3-D, from single-particle modeling methods to general particle modeling methods, the DEM model of particles has gradually improved. The contact models between soybean particles and the boundary mainly include the linear model, the nonlinear model, the Hertz model, the Hertz–Mindlin

model, and the visco-elastic contact model. The main test methods for verifying particle models include the bulk density test, angle of repose test, dynamic angle of repose test, silo discharge test, self-flow screening test, and rotating cylinder mixing test.

(2) For soil particle modeling, due to the complex composition, size and shape of soil particles, most scholars have used the single-sphere model to build their DEM models; some scholars have also built multi-sphere models of soil particles. The size of the particle model is determined according to the simulation needs. The main contact models used in analyzing soil particles include the parallel bonding model, the Edinburgh model, the HM+JKR model, etc. The main parameter calibration tests include the bulk density test, the cone penetration test, the angle of repose test, and compression and shear tests.

(3) Taking the seed throwing test of soybean as an example, when studying the interaction between particles with different material properties, the selection of the contact model and the calibration of the relevant parameters require careful analysis and study.

(4) For the simulation analysis of complex agricultural machinery, the DEM should be coupled with other algorithms, such as DEM and CFD coupling, DEM and MBD coupling, etc. These methods are mainly applied in the analysis of the sieving and seeding processes, but for the application of harvesting machinery, processing machinery, and in other fields, scholars still need to conduct in-depth research.

(5) In general, the DEM has been widely and successfully applied in the field of agricultural engineering, but the research aspect of DEM modeling for soil particles still faces great challenges, and has great research prospects, for example, soil particle modeling and particle parameter calibration, analysis of the seed throwing process, and parameter calibration between seeds, soil particles, etc., still need to be studied in depth.

Author Contributions: Conceptualization, D.Y.; methodology, D.Y.; validation, D.Y. and K.S.; investigation, Y.T. and resources, J.Y.; writing—original draft preparation D.Y.; writing—review and editing, Y.W.; supervision, L.Z.; project administration, J.Y.; funding acquisition, D.Y. All authors have read and agreed to the published version of the manuscript.

Funding: The authors are grateful to the National Natural Science Foundation of China (No. 52130001) for the financial support of this work.

Institutional Review Board Statement: Not applicable.

Informed Consent Statement: Not applicable.

Data Availability Statement: Not applicable.

Conflicts of Interest: The authors declare no conflict of interest.

References

1. Cundall, P.A.; Burman, B.C.; Strack, O.D.L. A discrete numerical model for granular assemblies. *Géotechnique* **1980**, *30*, 331–336. [CrossRef]
2. Dong, K.J.; Wang, B.; Yu, A.B. Modeling of Particle Flow and Sieving Behavior on a Vibrating Screen: From Discrete Particle Simulation to Process Performance Prediction. *Ind. Eng. Chem. Res.* **2013**, *52*, 11333–11343. [CrossRef]
3. Wang, Y.; Yu, J.Q.; Yu, Y.J. Validation of a coupled model of discrete element method with multibody kinematics to simulate the screening process of a swing-bar sieve. *Powder Technol.* **2019**, *346*, 193–202. [CrossRef]
4. Yu, Y.J.; Fu, H.; Yu, J.Q. DEM-based simulation of the corn threshing process. *Adv. Powder Technol.* **2015**, *26*, 1400–1409. [CrossRef]
5. Zeng, Z.W.; Ma, X.; Cao, X.L.; Li, Z.; Wang, X. Critical Review of Applications of Discrete Element Method in Agricultural Engineering. *Trans. Chin. Soc. Agric. Mach.* **2021**, *52*, 1–18.
6. Fang, H.M.; Ji, C.Y.; Chandio, F.A.; Guo, J.Z.Q.; Chaudhry, A. Analysis of Soil Dynamic Behavior during Rotary Tillage Based on Distinct Element Method. *Trans. Chin. Soc. Agric. Mach.* **2016**, *47*, 22–28.
7. Yu, J.Q.; Fu, H.; Li, H.; Shen, Y. Application of discrete element method to research and design of working parts of agricultural machines. *Trans. Chin. Soc. Agric. Eng.* **2005**, *21*, 1–6.
8. Lv, F.Y. *Investigation of Physical and Mechanical Properties and Modeling Method for Soybean Grains*; Jilin University: Changchun, China, 2017.

9. Shen, Y.F. *The Design for Precision Seed-metering Devices and Simulation Analysis of Working Process Based on the DEM*; Jilin University: Changchun, China, 2003.
10. Xu, Z. *Simulation Analysis of Collision Process of Soybean Based on the DEM*; Jilin University: Changchun, China, 2006.
11. Zhang, L.N. *Digital Design Method of Soybean Precision Seed-Metering Device Based on DEM*; Jilin University: Changchun, China, 2009.
12. Yu, J.Q.; Wang, G.; Xin, N.; Fu, H. Simulation Analysis of Working Process and Performance of Cell Wheel Metering Device. *Trans. Chin. Soc. Agric. Mach.* **2011**, *42*, 83–101.
13. Lu, Z.; Negi, S.C.; Jofriet, J.C. A Numerical Model for Flow of Granular Materials in Silos. Part 1: Model Development. *J. Agric. Eng. Res.* **1997**, *68*, 223–229. [CrossRef]
14. Nguyen, T.X.; Le, L.M.; Nguyen, T.C.; Nguyen, T.H.; Le, T.-T.; Pham, B.T. Characterization of soybeans and calibration of their DEM input parameters. *Part. Sci. Technol.* **2021**, *39*, 530–548. [CrossRef]
15. Vu-Quoc, L.; Zhang, X.; Walton, O.R. A 3-D discrete-element method for dry granular flows of ellipsoidal particles. *Comput. Methods Appl. Mech. Eng.* **1999**, *187*, 483–528. [CrossRef]
16. Boac, J.M.; Ambrose, R.P.K.; Casada, M.E.; Maghirang, R.G.; Maier, D.E. Applications of Discrete Element Method in Modeling of Grain Postharvest Operations. *Food Eng. Rev.* **2014**, *6*, 128–149. [CrossRef]
17. Boac, J.M.; Casada, M.E.; Maghirang, R.G.; Iii, J.P.H. Material and interaction properties of selected grains and oilseeds for modeling discrete particles. *Am. Soc. Agric. Biol. Eng.* **2000**, *54*, 1201–1216.
18. Tao, H.; Zhong, W.; Jin, B. Comparison of Construction Method for DEM Simulation of Ellipsoidal Particles. *Chin. J. Chem. Eng.* **2013**, *21*, 800–807. [CrossRef]
19. Liu, P.Y.; Yang, R.Y.; Yu, A.B. DEM study of the transverse mixing of wet particles in rotating drums. *Chem. Eng. Sci.* **2013**, *86*, 99–107. [CrossRef]
20. Xu, T.Y.; Yu, J.Q.; Yu, Y.J.; Wang, Y. A modelling and verification approach for soybean seed particles using the discrete element method. *Adv. Powder Technol.* **2018**, *29*, 3274–3290. [CrossRef]
21. Yan, D.X.; Yu, J.Q.; Wang, Y.; Long, Z.; Yu, Y.J. A general modelling method for soybean seeds based on the discrete element method. *Powder Technol.* **2020**, *372*, 212–226. [CrossRef]
22. Wang, X.M. *Study on Modeling Method of Maize Kernel Population Based on Multi—Ball Filling*; Jilin University: Changchun, China, 2017.
23. Kodama, M.; Rahul, B.; Curtis, J.; Hancock, B.; Wassgren, C. Force model considerations for glued-sphere discrete element method simulations. *Chem. Eng. Sci.* **2009**, *64*, 3466–3475. [CrossRef]
24. Kruggel-Emden, H.; Rickelt, S.; Wirtz, S.; Scherer, V. A study on the validity of the multi-sphere discrete element method. *Powder Technol.* **2008**, *188*, 153–165. [CrossRef]
25. Zhou, L.; Yu, J.; Wang, Y.; Yan, D.; Yu, Y. A study on the modelling method of maize-seed particles based on the discrete element method. *Powder Technol.* **2020**, *374*, 353–376. [CrossRef]
26. Lin, X.; Ng, T.T. Contact detection algorithms for three-dimensional ellipsoids in discrete element modeling. *Int. J. Numer. Anal. Methods Geomech.* **1995**, *19*, 653–659. [CrossRef]
27. Ouadfel, H.; Rothenburg, L. An algorithm for detecting inter-ellipsoid contacts. *Comput. Geotech.* **1999**, *24*, 245–263. [CrossRef]
28. Saini, N.; Kleinstreuer, C. A new collision model for ellipsoidal particles in shear flow. *J. Comput. Phys.* **2019**, *376*, 1028–1050. [CrossRef]
29. Barr, A.H. Superquadrics and Angle-Preserving Transformations. *IEEE Comput. Graph. Appl.* **1981**, *1*, 11–23. [CrossRef]
30. You, Y.; Zhao, Y.Z. Discrete element modelling of ellipsoidal particles using super-ellipsoids and multi-spheres: A comparative study. *Powder Technol.* **2018**, *331*, 179–191. [CrossRef]
31. Yan, D.; Yu, J.; Liang, L.; Wang, Y.; Yu, Y.; Zhou, L.; Sun, K.; Liang, P. A Comparative Study on the Modelling of Soybean Particles Based on the Discrete Element Method. *Processes* **2021**, *9*, 286. [CrossRef]
32. Di, R.A.; Di, M.F.P. An improved integral non-linear model for the contact of particles in distinct element simulations. *Chem. Eng. Sci.* **2005**, *60*, 1303–1312.
33. Landry, H.; Laguë, C.; Roberge, M. Discrete element representation of manure products. *Comput. Electron. Agric.* **2006**, *51*, 17–34. [CrossRef]
34. Gao, W.; Feng, Y.T. A coupled 3D discrete elements/isogeometric method for particle/structure interaction problems. *Comput. Part. Mech.* **2019**, *7*, 869–880. [CrossRef]
35. Horabik, J.; Beczek, M.; Mazur, R.; Parafiniuk, P.; Ryżak, M.; Molenda, M. Determination of the restitution coefficient of seeds and coefficients of visco-elastic Hertz contact models for DEM simulations. *Biosyst. Eng.* **2017**, *161*, 106–119. [CrossRef]
36. Chen, Z.; Wassgren, C.; Veikle, E.; Ambrose, K. Determination of material and interaction properties of maize and wheat kernels for DEM simulation. *Biosyst. Eng.* **2020**, *195*, 208–226. [CrossRef]
37. Wang, X.; Yu, J.; Lv, F.; Wang, Y.; Fu, H. A multi-sphere based modelling method for maize grain assemblies. *Adv. Powder Technol.* **2017**, *28*, 584–595. [CrossRef]
38. Mousaviraad, M.; Tekeste, M.Z.; Rosentrater, K.A. Calibration and Validation of a Discrete Element Model of Corn Using Grain Flow Simulation in a Commercial Screw Grain Auger. *Trans. ASABE* **2017**, *60*, 1403–1415. [CrossRef]
39. Wang, Y.; Lv, F.Y.; Xu, T.Y.; Yu, J. Shape and size analysis of soybean kernel and modeling. *J. Jilin Univ.* **2018**, *48*, 507–517.
40. Liu, F.Y.; Zhang, J.; Li, B.; Chen, J. Calibration of parameters of wheat required in discrete element method simulation based on repose angle of particle heap. *Trans. Chin. Soc. Agric. Eng.* **2016**, *32*, 247–253.

41. Coetzee, C.J. Particle upscaling: Calibration and validation of the discrete element method. *Powder Technol.* **2019**, *344*, 487–503. [CrossRef]
42. Cunha, R.; Santos, K.; Lima, R.; Duarte, C.R.; Barrozo, M. Repose angle of monoparticles and binary mixture: An experimental and simulation study. *Powder Technol.* **2016**, *303*, 203–211. [CrossRef]
43. Han, Y.; Zhao, D.; Jia, F.; Qiu, H.; Li, A.; Bai, S. Experimental and numerical investigation on the shape approximation of rice particle by multi-sphere particle models. *Adv. Powder Technol.* **2020**, *31*, 1574–1586. [CrossRef]
44. Coetzee, C.J.; Els, D.N.J. Calibration of discrete element parameters and the modelling of silo discharge and bucket filling. *Comput. Electron. Agric.* **2009**, *65*, 198–212. [CrossRef]
45. Xu, T.Y. *Expermental Study and Simulation Analysis of the Working Process of the Precision Seening Unit and Its Key Parts*; Jilin University: Changchun, China, 2019.
46. González-Montellano, C.; Ramírez, Á.; Gallego, E.; Ayuga, F. Validation and experimental calibration of 3D discrete element models for the simulation of the discharge flow in silos. *Chem. Eng. Sci.* **2011**, *66*, 5116–5126. [CrossRef]
47. Chen, Z.; Yu, J.; Xue, D.; Wang, Y.; Zhang, Q.; Ren, L. An approach to and validation of maize-seed-assembly modelling based on the discrete element method. *Powder Technol.* **2018**, *328*, 167–183. [CrossRef]
48. Cai, R.; Hou, Z.; Zhao, Y. Numerical study on particle mixing in a double-screw conical mixer. *Powder Technol.* **2019**, *352*, 193–208. [CrossRef]
49. Ma, H.; Zhao, Y. Modelling of the flow of ellipsoidal particles in a horizontal rotating drum based on DEM simulation. *Chem. Eng. Sci.* **2017**, *172*, 636–651. [CrossRef]
50. Gürsoy, S.; Chen, Y.; Li, B. Measurement and modelling of soil displacement from sweeps with different cutting widths. *Biosyst. Eng.* **2017**, *161*, 1–13. [CrossRef]
51. Ucgul, M.; Fielke, J.M.; Saunders, C. Three-dimensional discrete element modelling of tillage: Determination of a suitable contact model and parameters for a cohesionless soil. *Biosyst. Eng.* **2014**, *121*, 105–117. [CrossRef]
52. Ucgul, M.; Saunders, C.; Fielke, J.M. Discrete element modelling of top soil burial using a full scale mouldboard plough under field conditions. *Biosyst. Eng.* **2017**, *160*, 140–153. [CrossRef]
53. Bravo, E.L.; Tijskens, E.; Suárez, M.H.; Cueto, O.G.; Ramon, H. Prediction model for non-inversion soil tillage implemented on discrete element method. *Comput. Electron. Agric.* **2014**, *106*, 120–127. [CrossRef]
54. Zhang, Y.L. *Simulation and Experimental Study on Soil Throwing Performance of Reverse Rotation Fertilization Seeder Based on Discrete Element Method*; Jiangsu University: Zhenjiang, China, 2012.
55. Pan, S.Q. *Research on the Optimization Design and the Experiment of the Core Ploughshare Furrow Opener Based on the Discrete Element Method*; Jilin University: Changchun, China, 2015.
56. Yan, D.X. *Particle Modelling of Soybean Seeds and The Simulation Analysis and Experimental Study of the Seed-Throwing and Pressing*; Jilin University: Changchun, China, 2021.
57. Milkevych, V.; Munkholm, L.J.; Chen, Y.; Nyord, T. Modelling approach for soil displacement in tillage using discrete element method. *Soil Tillage Res.* **2018**, *183*, 60–71. [CrossRef]
58. Chen, Y.; Munkholm, L.J.; Nyord, T. A discrete element model for soil–sweep interaction in three different soils. *Soil Tillage Res.* **2013**, *126*, 34–41. [CrossRef]
59. Obermayr, M.; Vrettos, C.; Eberhard, P.; Däuwel, T. A discrete element model and its experimental validation for the prediction of draft forces in cohesive soil. *J. Terramech.* **2014**, *53*, 93–104. [CrossRef]
60. Ma, Y.J.; Wang, A.; Zhao, J.G.; Hao, J.; Li, J.; Ma, L.; Zhao, W. Simulation analysis and experiment of drag reduction effect of convex blade subsoiler based on discrete element method. *Trans. Chin. Soc. Agric. Eng.* **2019**, *35*, 16–23.
61. Wang, X.L.; Hu, H.; Wang, Q.G.; Li, H.; He, J.; Chen, W. Calibration Method of Soil Contact Characteristic Parameters Based on DEM Theory. *Trans. Chin. Soc. Agric. Mach.* **2017**, *48*, 78–85.
62. Xiang, W.; Wu, M.L.; Lü, J.N.; Quan, W.; Ma, L.; Liu, G. Calibration of simulation physical parameters of clay loam based on soil accumulation test. *Trans. Chin. Soc. Agric. Eng.* **2019**, *35*, 116–123.
63. Wu, T.; Huang, W.F.; Chen, X.S.; Ma, X.; Han, Z.Q.; Pan, T. Calibration of discrete element model parameters for cohesive soil considering the cohesion between particles. *J. South China Agric. Univ.* **2017**, *38*, 93–98.
64. Shi, L.R.; Zhao, W.Y.; Sun, W. Parameter calibration of soil particles contact model of farmland soil in northwest arid region based on discrete element method. *Trans. Chin. Soc. Agric. Eng.* **2017**, *33*, 181–187.
65. Xie, F.P.; Wu, Z.Y.; Wang, X.S.; Liu, D.; Wu, B.; Zhang, Z. Calibration of discrete element parameters of soils based on unconfined compressive strength test. *Trans. Chin. Soc. Agric. Eng.* **2020**, *36*, 39–47.
66. Li, J.W.; Tong, J.; Hu, B.; Wang, H.; Mao, C.; Ma, Y. Calibration of parameters of interaction between clayey black soil with different moisture content and soil-engaging component in northeast China. *Trans. Chin. Soc. Agric. Eng.* **2019**, *35*, 130–140.
67. Wang, X.; Zhang, Q.; Fu, Z.; Wei, W.; He, J.; Huang, Y. An efficient method for determining DEM parameters of a loose cohesive soil modelled using hysteretic spring and linear cohesion contact models. *Biosyst. Eng.* **2022**, *205*, 283–294. [CrossRef]
68. Lin, J.; Bao, M.; Zhang, F.; Yang, J.; Li, H. Mixing simulation of cohesive particles in a soil mixer. *Powder Technol.* **2022**, *399*, 117–218. [CrossRef]
69. Bufton, L.P.; Richardson, P.; O'Dogherty, M.J. Seed displacement after impact on a soil surface. *J. Agric. Eng. Res.* **1974**, *19*, 327–338. [CrossRef]

70. Ma, X.; Yu, H.Y.; Yang, H.K. The determining and model establishing of seed bouncing and rolling displacement after impact on a furrow. *Trans. Chin. Soc. Agric. Mach.* **1998**, *29*, 58–62.
71. Ma, C.L. *Precision Seeding Theory*; Jilin Science and Technology Press: Changchun, China, 1999.
72. Wang, Y.S.; Zheng, D.C.; Wu, H.P.; Wu, H. Probability Distribution of Seed Spacing of Precision Drilling. *Trans. Chin. Soc. Agric. Mach.* **2001**, *32*, 40–43.
73. Sui, J. *Research on Experiment and Simulation Analysis of Soybean Collision with Soil*; Jilin University: Changchun, China, 2016.
74. Hao, J.J.; Long, S.F.; Li, H.; Jia, Y.; Ma, Z.; Zhao, J. Development of discrete element model and calibration of simulation parameters for mechanically-harvested yam. *Trans. Chin. Soc. Agric. Eng.* **2019**, *35*, 34–42.
75. Dowding, C.H.; Belytschko, T.B.; Yen, H.J. A coupled finite element–rigid block method for transient analysis of rock caverns. *Int. J. Numer. Anal. Methods Geomech.* **2010**, *7*, 117–127. [CrossRef]
76. Dowding, C.H.; Gilbert, C. Dynamic Stability of Rock Slopes and High Frequency Traveling Wave. *J. Geotech. Eng.* **1989**, *114*, 1069–1088. [CrossRef]
77. Michael, M.; Vogel, F.; Peters, B. DEM–FEM coupling simulations of the interactions between a tire tread and granular terrain. *Comput. Methods Appl. Mech. Eng.* **2015**, *289*, 227–248. [CrossRef]
78. Ding, L.; Yang, L.; Wu, D.H.; Li, D.; Zhang, D.; Liu, S. Simulation and Experiment of Corn Air Suction Seed Metering Device Based on DEM CFD Coupling Method. *Trans. Chin. Soc. Agric. Mach.* **2018**, *49*, 48–57.
79. Ren, B.; Zhong, W.; Chen, Y.; Chen, X.; Jin, B.; Yuan, Z.; Lu, Y. CFD-DEM simulation of spouting of corn-shaped particles. *Particuology* **2012**, *10*, 562–572. [CrossRef]
80. Yang, W. *Simulation Analysis and Experimental Study of the Screening Process of a Swing-Bar Sieve Based on the Coupling of DEM with MBK*; Jilin University: Changchun, China, 2018.
81. Yuan, J.; Yu, J.Q. Analysis on Operational Process of Self-excited Vibrating Subsoiler Based on DEM-MBD Coupling Algorithm. *Trans. Chin. Soc. Agric. Mach.* **2020**, *51*, 17–24.
82. Zhang, L.; Zhai, Y.; Chen, J.; Zhang, Z.; Huang, S. Optimization design and performance study of a subsoiler underlying the tea garden subsoiling mechanism based on bionics and EDEM. *Soil Tillage Res.* **2022**, *220*, 105375. [CrossRef]